CONSTRAINTS ON UNROOFING RATES IN THE HIGH
HIMALAYA, EASTERN NEPAL

Mary Hubbard[1], Leigh Royden, and Kip
Hodges

Department of Earth, Atmospheric, and
Planetary Sciences, Massachusetts
Institute of Technology, Cambridge

Abstract. Thermobarometric data for
samples across the Main Central thrust
zone in eastern Nepal show an inversion in
temperature but not in pressure. These
data have been interpreted to represent a
portion of the paleogeotherm at the time
of Main Central thrust deformation. A
40Ar/39Ar age on hornblende (closure
temperature (Tc)=500 ± 50°C) constrains
the timing of this deformation to be
~21±0.2 Ma. The 40Ar/39Ar ages of other
minerals (muscovite, Tc=350°C, age (t)
=12.0±0.2 Ma; K-feldspar, Tc=220°C,
t=8.0±0.2 Ma) from the same location
further constrain the cooling history of
this region. Together the geochronologic
and thermobarometric data yield an average
unroofing rate of 1.2±0.6 mm/yr for the
High Himalaya of eastern Nepal.

Simple thermal models show that these
geochronologic and thermobarometric data
are consistent with a wide range of
different initial geotherms, applied
boundary conditions and magnitude of
radiogenic heat production. The variation
through time of the unroofing rates can
only be poorly constrained, however. The
unroofing histories were found to be
largely insensitive to the details of the
assumed initial geotherm, fairly sensitive
to the magnitude of radiogenic heat
production, and extremely sensitive to the
nature of the boundary conditions applied
below the fault zone. This study
underscores the difficulty in constraining
uplift histories on the basis of cooling
rates even when thermobarometric data are
available to supplement geochronologic
constraints on the cooling history of the
region.

INTRODUCTION

The Himalayan mountain belt is the
highest and arguably the most spectacular
example of continent-continent collision
in the world. Of particular interest is
the structural and metamorphic development
of the Main Central Thrust (MCT), a major
north dipping thrust fault that is
believed to have accommodated much of the
postcollisional convergence within the
Himalaya. Hubbard [1988] generated
pressure-temperature-time (PTt) data for
rocks collected adjacent to the MCT zone
in eastern Nepal. These data provide
important constraints on the synkinematic
and postkinematic cooling and unroofing
history of the MCT zone and thus allow
control on thermal models for this
midcrustal thrust fault.

In recent years a host of theoretical

[1]Now at Department of Geological
Sciences, University of Maine, Orono.

models have been constructed in an attempt
to understand the thermal response of the
lithosphere to collisional orogenesis
[e.g., England and Richardson, 1977;
Oxburgh and Turcotte, 1974; Royden and
Hodges, 1984; Molnar and England, 1990].
Most of these are loosely constrained by
qualitative observations of metamorphic
grade, and lack quantitative data on
temperature, pressure, or time. Other
studies have used geochronologic data
together with assumptions of the
geothermal gradient to constrain erosion
histories [Zeitler, 1985; Copeland et al.,
1987]. For the High Himalaya in eastern
Nepal we have time-temperature data that
provide constraints on the cooling history
of a structural horizon and pressure-
temperature data that provide constraints
on an initial geotherm. In our study we
use this combined data set to assess our
ability to constrain unroofing rates
through time in an evolving orogenic belt
in which movement along midcrustal thrust
faults has played a major role in crustal
shortening and thickening. Unfortunately,
even with petrologic and geochronologic
constraints there is sufficient
uncertainty in radiogenic heat production,
deep crustal structure, and the PTt data
themselves to inhibit high resolution
determination of the unroofing history.

TECTONIC SETTING AND PTt DATA BASE

    Following continental collision at
about 50 Ma [Molnar, 1984],
postcollisional convergence in the
Himalaya has resulted in two major north
dipping thrust faults, the MCT and the
Main Boundary Thrust (MBT). Both thrust
faults are laterally continuous for nearly
2000 km along the length of the Himalaya
(Figure 1). Based on the position of
structural windows and outlying klippen,
estimates of the minimum displacement
across these faults are ~100 km for the
MCT and ~35 km for the MBT. Along most of
the Himalaya the MCT juxtaposes high-grade
metamorphic rocks in its hanging wall
against lower grade sedimentary and
metasedimentary rocks in its footwall
[Gansser, 1964]. In eastern Nepal the MCT
is a zone 3-5 km thick comprised of a
sheared sequence of variable lithology
containing medium- to high-grade, garnet-
bearing rocks [Hubbard, 1988]. The
metamorphic grade increases up section
(northward) across this zone from garnet-

staurolite grade in the lower MCT zone
through kyanite-bearing rocks to
sillimanite-bearing rocks in the upper MCT
zone and the overlying sequence, the
Tibetan Slab.
    Hubbard [1988] generated
thermobarometric and 40Ar/39Ar
geochronologic data for a suite of samples
collected on two transects across the MCT
zone and Tibetan Slab (Figure 1b).
Thermobarometric data were generated for
mineral rims using the garnet-biotite
geothermometer [Ferry and Spear, 1978] and
three geobarometers (garnet-aluminum
silicate-quartz-plagioclase [Newton and
Haselton, 1981], garnet-muscovite-
plagioclase-biotite [Hodges and Crowley,
1985], and garnet-rutile-aluminum
silicate-ilmenite [Bohlen et al., 1983].
The timing of major movement along the MCT
and its subsequent cooling history are
constrained by 40Ar/39Ar cooling ages for
hornblende (20.9±0.2 Ma), muscovite
(12.0±0.2 Ma) and K-feldspar (8.0±0.2 Ma)
mineral separates from the lowermost unit
within the MCT zone [Hubbard and Harrison,
1989]; all uncertainties are reported at
the 95% confidence level. The hornblende
and muscovite ages are isochron ages, and
the K-feldspar age is the minimum age on
its release spectrum.
    When thermometric data are plotted
against structural distance across the MCT
zone and into the Tibetan Slab above
(Figure 2a), it can be seen that
metamorphic temperatures first increase
upwards from the lowermost MCT zone to a
structural horizon ~2 km above the top of
the MCT zone and then decrease upwards to
a structural horizon ~7 km above the top
of the MCT zone [Hubbard, 1989]. In a
similar plot, metamorphic pressure data
from this study show scatter but generally
outline a decrease in pressure upward
within the MCT zone and the deepest part
of the Tibetan Slab (Figure 2b). The
slope indicated by a simple least squares
linear regression of the pressure data
versus structural position is ~28 MPa/km,
or approximately a lithostatic pressure
gradient. Although the uncertainty in
this slope is large, a similar gradient
was obtained by Hodges et al. [1988] for a
suite of samples from MCT zone and Tibetan
Slab in central Nepal. We follow Hodges
et al. [1988] in interpreting the
preservation of a roughly lithostatic
pressure profile to mean that all of the
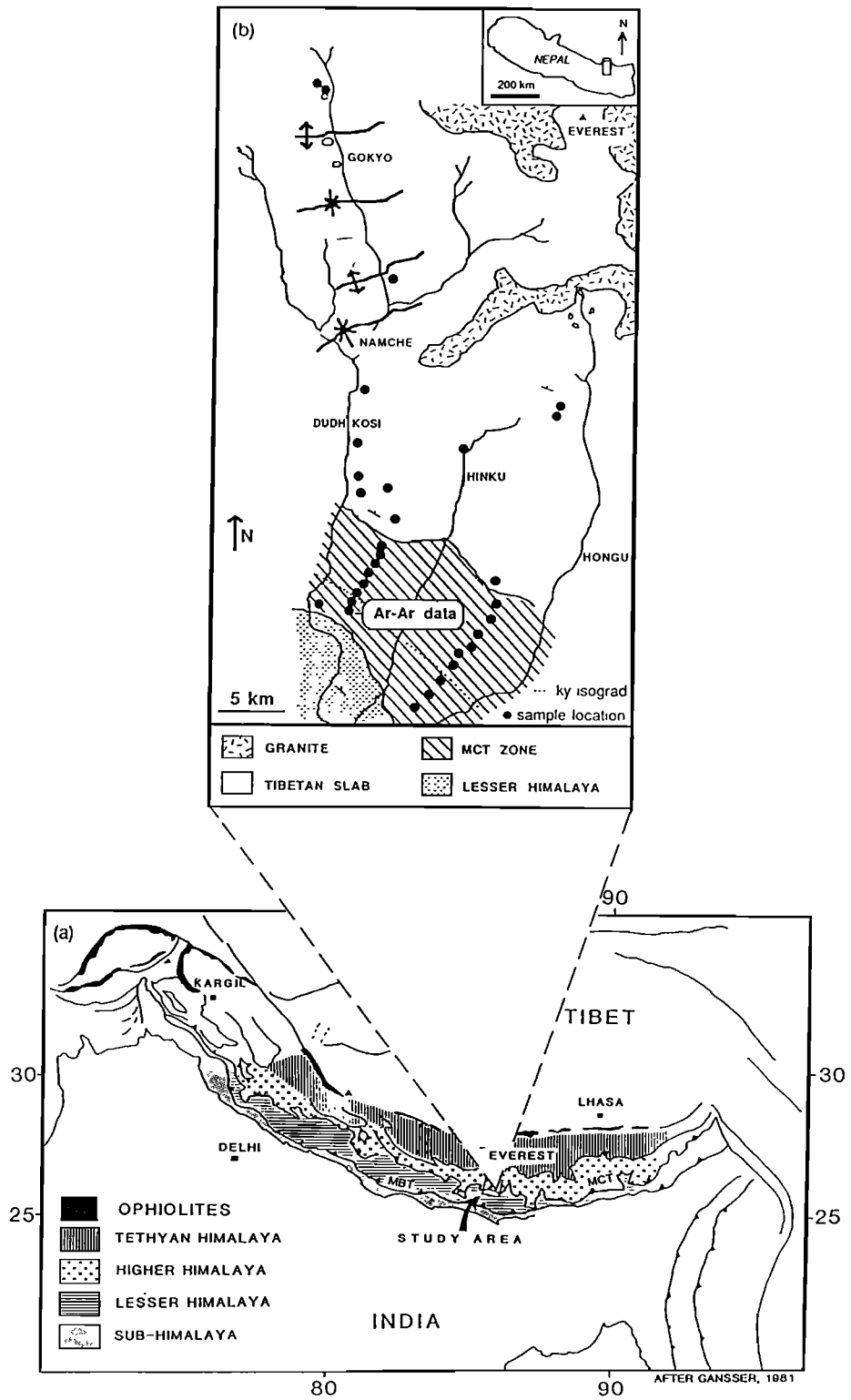samples equilibrated at approximately the
same time.

Fig. 1. (a) Simplified geologic map of the Himalaya [after Gansser, 1981]; (b) geologic map of the study area showing locations of samples used for thermobarometry (solid dots) and 40Ar/39Ar geochronometry.

(a)

(b)

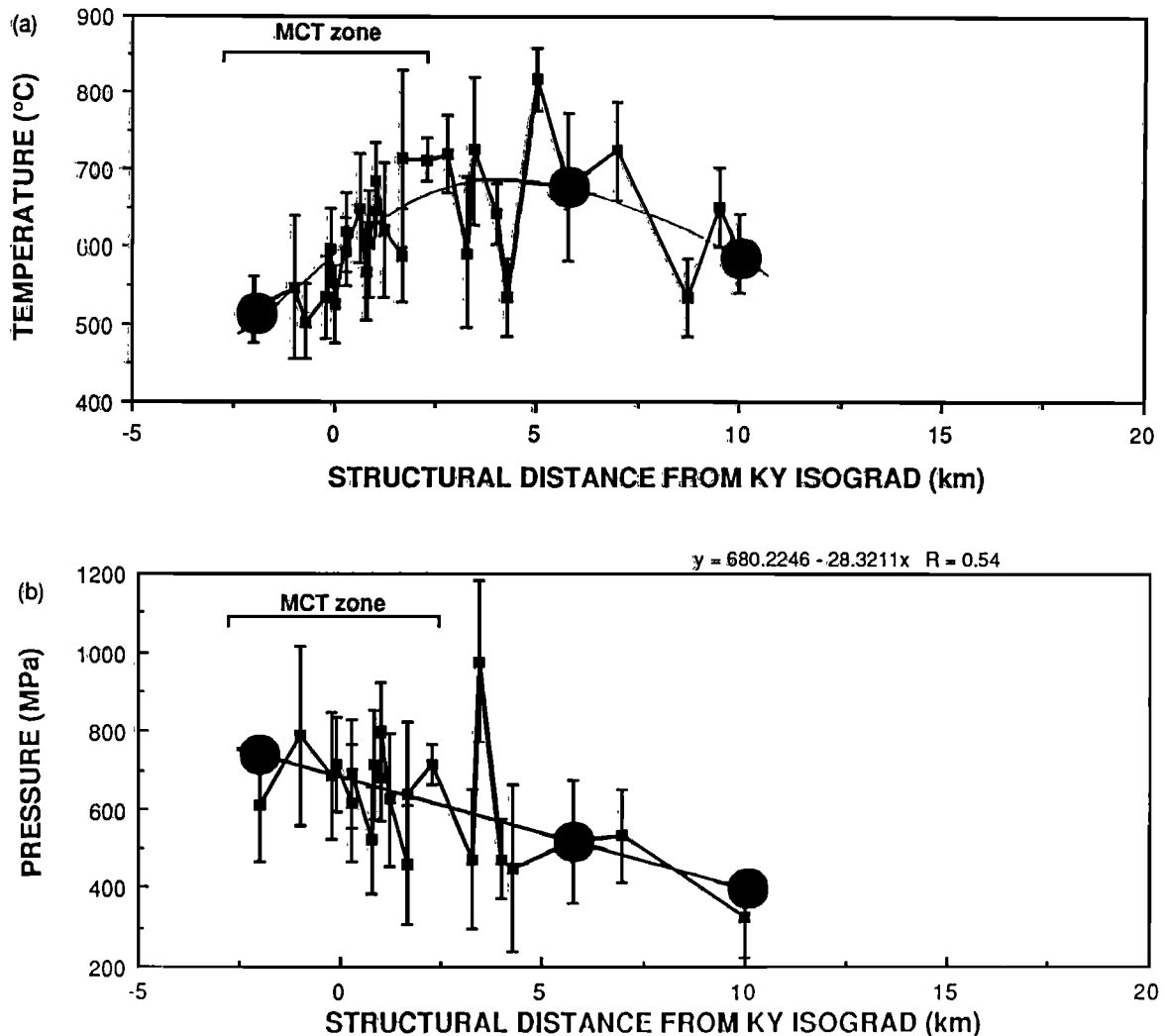$y = 680.2246 - 28.3211x \quad R = 0.54$

Fig. 2. (a) Summary of thermometric data from the MCT zone and lower Tibetan Slab; (b) barometric data from the MCT zone and lower Tibetan Slab. Precision limits are shown at the 95% confidence level. Large solid dots denote P-T conditions used to constrain the upper 26 km of the initial geotherm.

The pressure and temperature trend relative to structural position (i.e., an approximately lithostatic pressure gradient coincident with inverted temperatures) together with metamorphic textures has led to the interpretation that the metamorphism was synchronous with at least one episode of thrusting along this portion of the MCT [Hubbard, 1989]. If this interpretation is correct, the lithostatic pressure gradient and syndeformational nature of the metamorphism within the MCT zone and lowermost Tibetan slab suggest that the

metamorphic pressures recorded for each sample were probably recorded just prior to the end of thrusting. If this were not the case, shearing within the MCT zone would have juxtaposed rocks which equilibrated at different depths, and the observed pressure profiles would not be expected to mimic a lithostatic gradient. Provided that the metamorphic temperatures were recorded at the same time as the metamorphic pressures, the metamorphic temperatures recorded in these samples outline an approximate paleogeotherm because they represent temperatures

recorded at approximately the same time within a column of crustal material [cf. Hodges et al., 1988].

Because the hornblende closure temperature (~500°C [Harrison, 1981]) falls within the range of metamorphic temperatures calculated for the lower part of the MCT zone, Hubbard and Harrison [1989] interpreted the hornblende age of 21 Ma as approximately the age of metamorphism and thrusting. (Rigorous uncertainties for closure temperature are undetermined but are generally assumed to be within 50°-75°C; see Hodges [1991] for a discussion). Comparison of the PT data shown in Figures 2a and 2b reveals that this age corresponds to a metamorphic pressure of 730±100 MPa, or about 26±4 km. Note that the uncertainties in Figures 2a and 2b reflect analytical precision rather than the accuracy of pressure and temperature estimates; rigorous propagation of all sources of error associated with thermobarometry would lead to depth uncertainties of the order of 10 km [Hodges and McKenna, 1987]. For modeling purposes we will assume that the late stages of shear within the MCT zone occurred at about 21 Ma at a depth of about 26 km. The estimated absolute pressure (730 MPa) is consistent with the observed structural thickness of the upper plate. Cooling ages for muscovite and K-feldspar, with closure temperatures of 350°C and 220°C respectively [Harrison and McDougall, 1980], yield further contraints on the postthrusting cooling history of the lower part of the MCT zone and indirect constraints of the unroofing history.

In summary, we interpret the PT data recorded within and above the MCT zone in eastern Nepal to represent a paleogeotherm at approximately 21 Ma, when the lower part of the MCT zone was at a depth of 26 km. Isotopic cooling ages from the lower part of the MCT zone show that cooling of these rocks reduced the temperature of this zone to 350°C by 12 Ma and to 220°C by 8 Ma, and this horizon is now exposed at the surface. Over the last 21 Ma, the temperature within the lower part of the MCT zone must never have exceeded ~500°C for any significant length of time because this would have reset the 40Ar/39Ar isotopic clock for hornblende as well as the garnet-biotite geothermometer.

In the following sections we use heat transfer calculations to (1) establish that some combination of initial geotherm

(at 21 Ma) and unroofing rate are compatible with the PTt data from the MCT zone in eastern Nepal and (2) define the confidence with which the geotherm at 21 Ma and changes in the unroofing rate (as a function of time) can be constrained by the available data. The second point is particularly important because unroofing rates in eroding orogenic belts are commonly defined by cooling rates alone, and are usually assumed to be linearly related to them. While this assumption is clearly incorrect, the set of PTt data from eastern Nepal will allow us to test to what extent this approach may yield at least a very qualitative picture of unroofing history.

METHOD AND ASSUMPTIONS

The deformational history above and below the MCT is uncertain from 21 Ma to present. Small shear zones do exist above the MCT and 40Ar/39Ar ages constrain the timing of deformation in one shear zone to be ~8-12 Ma. Broad folding in eastern Nepal also postdates MCT movement, as does thrusting below the MCT (i.e., the MBT). We don't know, however, what the thermal significance is of post-MCT deformation. We have addressed thrusting below the MCT (see second scenario below), but we have assumed thermal effects of other deformation to be minor, and therefore such effects have not been considered in our modeling.

We consider two end-member possibilities in setting up our thermal boundary conditions for the evolving temperature structure of the MCT. Although neither of these is likely to be absolutely correct, we feel that the two scenarios illustrate the wide range of possibilities in assigning boundary conditions within this orogenic belt. In the first instance, we assume that there was no movement on any structurally lower faults (e.g., the MBT) during most of the uplift history of the MCT zone. This means that from 21 Ma to the present, India-Asia convergence must have been accommodated by deformation north of the Himalaya. For simplicity we assume that deformation occurred north of the region sampled in this study and did not involve rocks in the hanging wall of the MCT. We can thus treat the problem as if there were no deformation of the lithosphere above or below the MCT after 21 Ma. (We note that there was clearly thrusting at

the foot of the Himalaya by Pliocene time [e.g., Lyon-Caen, and Molnar, 1985], but this postdates the recording of our last isotopic age at 8 Ma.)

In the second instance we assume that a deeper thrust fault (the MBT?) became active immediately following the cessation of thrusting on the MCT at 21 Ma. For simplicity we assume that this fault lies 15 km below the MCT in the region studied, equivalent to the present depth of the MBT at the latitude of the study area today.

In both structural scenarios we chose an estimated geotherm that was compatible with the PT data obtained from eastern Nepal and considered this to be the geotherm at 21 Ma (we will refer to this as the initial geotherm). We used a finite difference approximation to the one-dimensional heat flow equation [Carslaw and Jaeger, 1959; Carnahan et al., 1969] to chart the temperature-time history of the lower MCT zone, assuming that there was no deformation during cooling except for surface erosion (or tectonic denudation) at some specified rate. Because it is impossible to constrain anything other than the average uplift rate between 21 and 12 Ma, between 12 and 8 Ma, and between 8 and 0 Ma (corresponding to cooling ages of the various mineral systems), the rate of surface erosion was assumed to be constant over each of these intervals. The rate of surface erosion during each of these intervals was then adjusted by trial and error until the temperature of the lower MCT zone cooled through $350°±50°C$ at 12 Ma, through $220°±30°C$ at 8 Ma, and through $0°C$ at 0 Ma when it reached the surface. In addition, we required the temperature of the lower MCT zone to remain less than about $500°C$ at all times so as not to reset the Ar isotopic clock in amphibole.

Note that in making these computations of time-dependent unroofing rate we ignore errors and uncertainties in the observed PT data and consider only the nominal values without uncertainties. Clearly the inclusion of these uncertainties will increase the range of possible unroofing histories computed, but as will become clear in the following sections this should have little effect on the main results of this study.

For the structural scenario with no deformation above or below the MCT we treated the lithosphere as a slab of constant thickness (120 km) with constant temperature at its surface ($0°C$) and base

($1300°C$). Erosion or removal of material at the surface was simulated by allowing the surface isotherm at $0°C$ to move downward through the temperature grid at the rate of erosion while the base of the lithosphere at $1300°C$ moved downward at the same rate, thus maintaining the $1300°C$ basal temperature and 120 km thickness. (Note that boundary conditions at 120 km depth or deeper require at least 50 m.y. to have an effect on temperatures near the surface so that the exact nature of the lower boundary conditions chosen are not important.) Initial temperatures within the upper portion of the lithosphere (within and above the MCT zone) are fairly well constrained by three pressure-temperature (P-T) points as shown in Figures 2 and 3, but at depths greater than 26 km the initial geotherm is not constrained by PT data directly. Therefore several possibilities for the initial geotherm in the deeper crust and mantle were assumed (Figure 3). These geotherms resemble the "sawtooth" form that has been suggested for one-dimensional models of instantaneous overthrusting [Oxburgh and Turcotte, 1974; England and Thompson, 1984].

For the structural scenario that includes continuous movement on a thrust fault 15 km below the MCT, we assume a roughly constant temperature of $275°C$ across this structurally deeper fault from 21 Ma until the present. The purpose of this exercise is to test the sensitivity of our assumed thermal boundary conditions on the computed thermal structure and unroofing rate of the Himalayas in eastern Nepal; we do not mean to imply that we can define the temperatures or boundary conditions below the MCT with any precision. In this case the initial geotherm is almost completely specified by the three P-T points and by requiring the temperature of $275°C$ at a depth 15 km below the MCT (initial geotherm "d" in Figure 3). (A similar approach has been used for a thermal model of the central Alps [Bradbury and Nolen-Hoeksema, 1985].)

Radiogenic heat production was assumed to be uniformly distributed throughout a layer that is initially 50 km thick and thins accordingly during erosion. Because the magnitude of the radiogenic heat production in the Himalaya is not well constrained, a range of values for heat production was considered: 0, 1.0, 2.0, and 3.0 $\mu W/m^3$ [England and Thompson, 1984]. In this way we can examine the

TEMPERATURE (C)
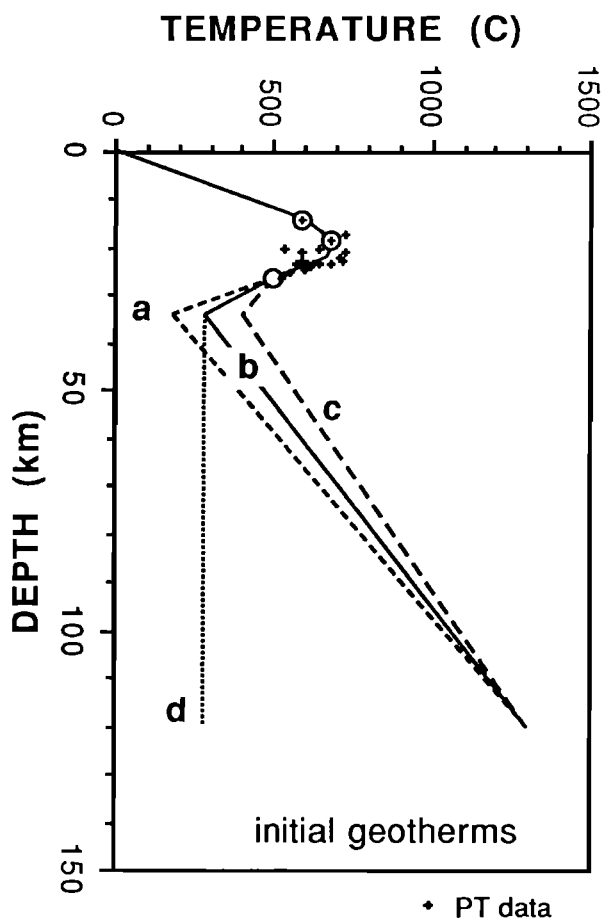

initial geotherms

• PT data

Fig. 3. Initial geotherms a-d. Crosses represent temperature data as a function of structural position and open circles represent the three P-T points used to constrain the upper 26 km of the initial geotherms.

sensitivity of our results to the magnitude of heat production. Thermal diffusivity was taken to be 10-6 m2/s.

RESULTS

The first and most basic result of this study is obtained without the need for thermal modeling. Assuming that the depth of the lower MCT was 26±10 km at 21±0.2 Ma and that it is now exposed at the surface, the average unroofing rate of the MCT since 21 Ma is 1.2±0.6 km/m.y.. This result is independent of the initial geotherm or the thermal boundary conditions assumed.

In order to analyze how this average

unroofing rate is distributed through time we first modeled the thermal history of the MCT assuming that the initial geotherm corresponded to geotherm "b" in Figure 3. Figure 4 shows the calculated temperature-time history for the lower part of the MCT zone assuming constant unroofing rates of 1.5, 1.75, and 2.0 km/m.y. This first set of calculations was made with a radiogenic heat production of 3.0 μW/m3 because such high values have been reported in the Himalaya [Pinet and Jaupart, 1987]. Unroofing rates of 2.0 and 1.75 km/m.y. are clearly acceptable between 21 and 12 Ma but fail to match the temperature-time observations at 8 Ma and at 0 Ma. Therefore the unroofing rate must change through time to satisfy both the thermobarometric and geochronologic data. An unroofing rate of 1.5 km/m.y. is too slow (for initial geotherm "b") to fit the observations at 12 Ma, and rates much faster than 2.0 km/m.y. will also not fit these observations. Setting the unroofing rate between 21 and 12 Ma equal to 1.85 km/m.y. (which passes through the midpoint of the temperature-time observation at 12 Ma), this trial and error technique was repeated to establish an acceptable unroofing rate of 1.0 km/m.y. between 12 Ma and 8 Ma, and of 0.7 km/m.y. between
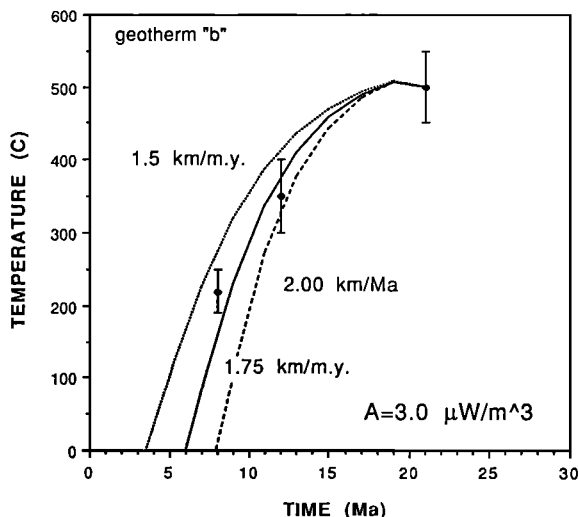

TIME (Ma)

Fig. 4. T-t paths for initial geotherm "b" assuming constant unroofing rates. The $^{40}Ar/^{39}Ar$ data points are shown with estimated uncertainties in closure temperatures. Radiogenic heat production = 3.0 μW/m3.

8.0 Ma and 0 Ma (Figure 5). Note that at
12 Ma the cooling rate increases while the
unroofing rate decreases, underscoring the
point that unroofing rate and cooling rate
need not be (and usually are not)
proportional to one another. Despite the
success of the calculated Tt path shown in
Figure 5 in fitting the cooling ages and
initial PT conditions observed in the MCT
zone this path violates our assumption
that the sample never experience
temperatures above the hornblende closure
temperature after 21 Ma. Thus geotherm
"b" with A = 3.0 µW/m3 does not provide an
acceptable solution for the evolving
thermal structure of the Himalaya in
eastern Nepal.

Figure 6 shows the results obtained
using initial geotherm "b" and varying the
radiogenic heat production from 0 to 2.0
µW/m3. Unlike the temperature-time path

Fig. 6. (a) T-t paths derived from initial
geotherm "b" for radiogenic heat
production values of 0, 1.0, and 2.0
µW/m3; (b) unroofing rates used to
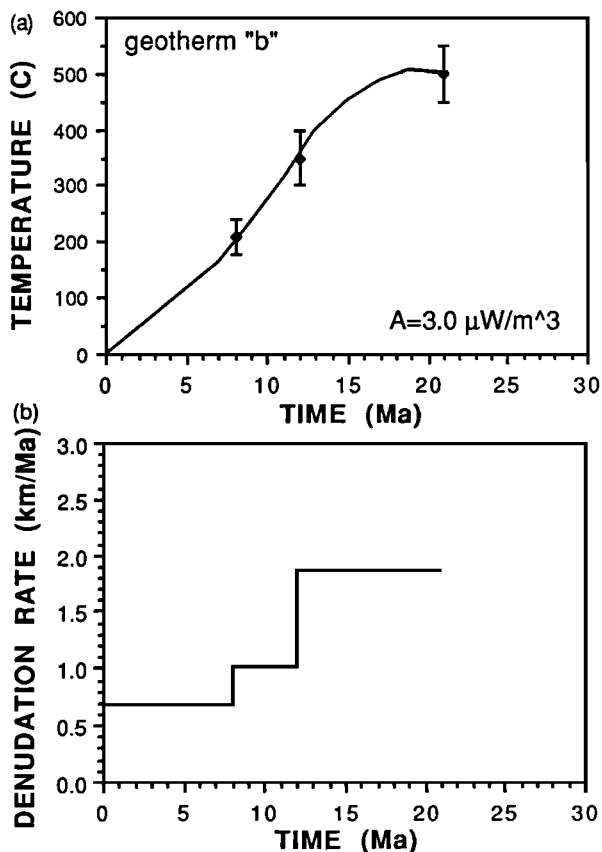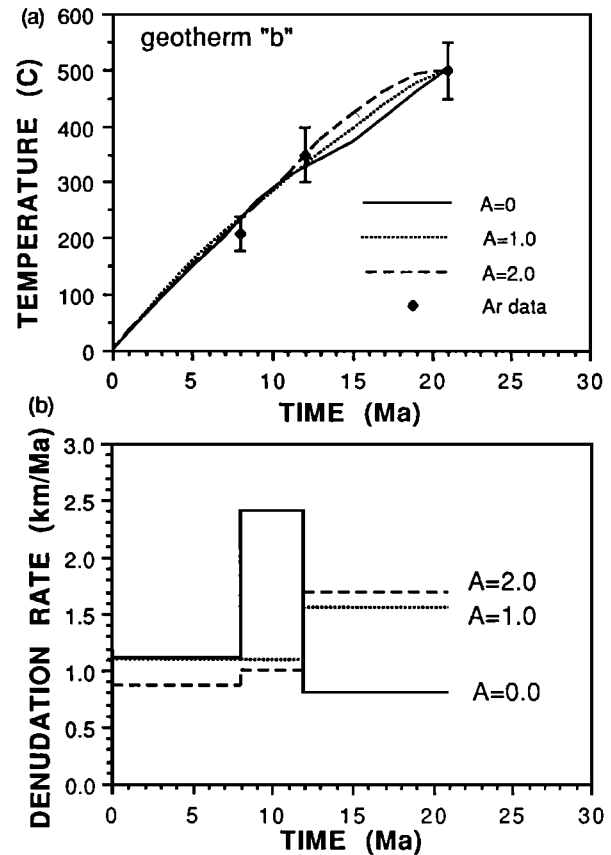calculate the T-t paths shown in Figure
6a.

Fig. 5. (a) T-t path derived from varying
unroofing rates for initial geotherm "b";
(b) unroofing rates used to calculate the
T-t path shown in Figure 5a. Radiogenic
heat production = 3.0 µW/m3.

calculated with higher values of
radiogenic heat production, these paths
satisfy the observed Tt and PT conditions
and do not violate the assumption that the
samples never experience temperatures in
excess of the hornblende closure
temperature after 21 Ma. Figure 6 also
shows that the calculated unroofing
history is strongly dependent on the
magnitude of radiogenic heat production,
especially between 21 and 12 Ma when
calculated unroofing rates vary between
about 0.8 and 1.7 km/m.y., and between 12
and 8 Ma when unroofing rates vary between
about 1 and 2.5 km/m.y. Similar
variations in unroofing rate are obtained
when geotherms "a" and "c" are used to
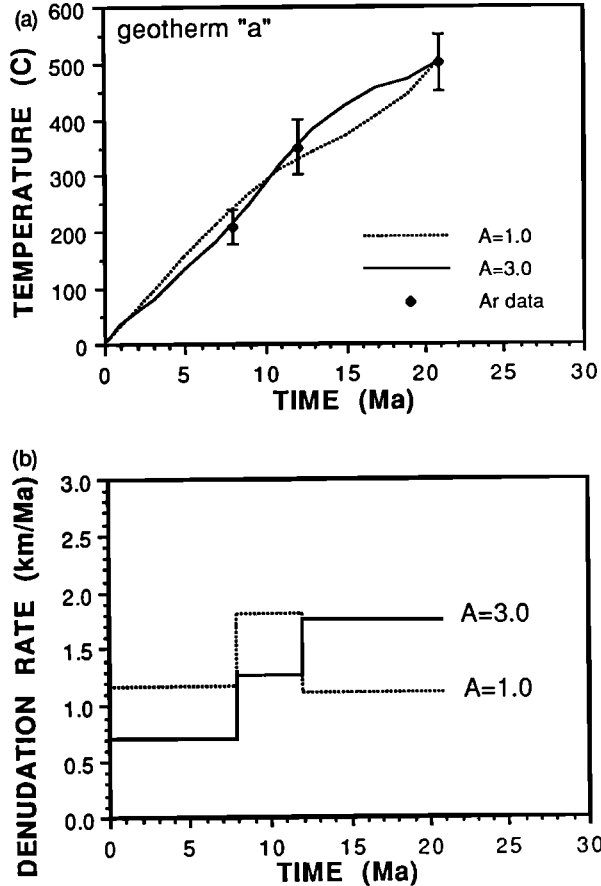constrain the initial temperatures
(Figures 7 and 8).

Fig. 7. (a) T-t paths derived from initial
geotherm "a" for radiogenic heat
production values of 1.0 and 3.0 μW/m3;
(b) unroofing rates used to calcualte the
T-t paths shown in Figure 7a.

Fig. 8. (a) T-t paths derived from initial
geotherm "c" for radiogenic heat
production values of 1.0 and 3.0 μW/m3;
(b) unroofing rates used to calculate the
T-t paths shown in Figure 8a.

We used the same approach to compute an
unroofing history generated by a geotherm
that initially passed through the three
pressure-temperature points and was also
constrained at all times to be 275°C at a
point 15 km below the MCT (see discussion
in previous section). With an assumed
radiogenic heat production of 1.0 μW/m3
the sample cools too quickly to pass
through the temperature-time constraint at
12 Ma, even without removal of any
material at the surface (Figures 9a and
9b). When the radiogenic heat production
is taken to be 3.0 μW/m3, the calculated
temperature-time path is in good agreement
with the observations for an unroofing
rate of 0.25 km/m.y. from 21 Ma to 12 Ma,
2.75 km/m.y. from 12 Ma to 8 Ma, and 1.3
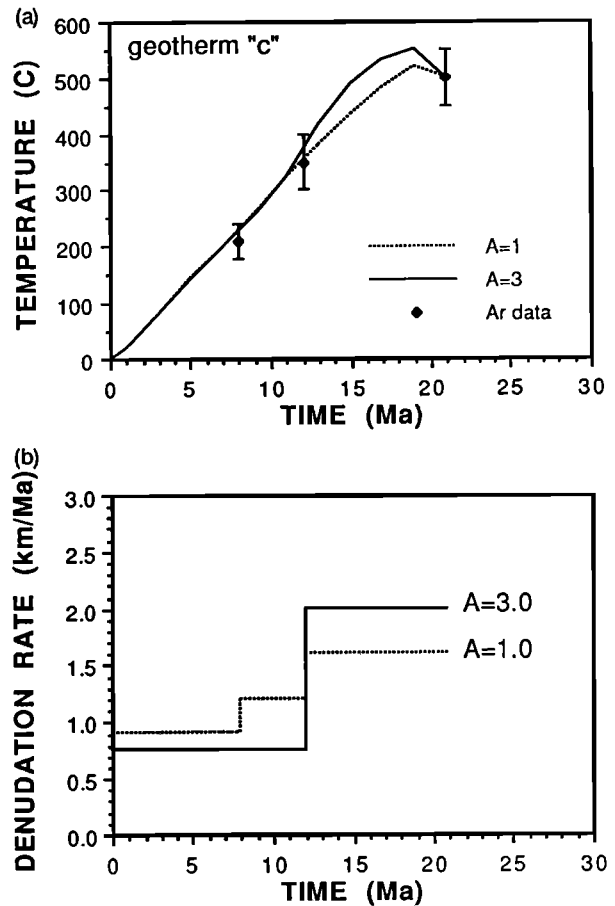km/m.y. from 8 Ma to 0 Ma.

DISCUSSION

While the average rate of unroofing of
the MCT zone in eastern Nepal is
constrained to have been 1.2±0.6 km/m.y.
over the time interval from 21 Ma to
present, the way in which that unroofing
is partitioned through time can be only
poorly determined. Thus the roughly
constant cooling rate observed for samples
from the MCT is compatible with unroofing
rates that increase greatly through time
(geotherm "d"), with unroofing rates that
decrease greatly through time (geotherm
"b", A=3 mW/m3), and with unroofing rates
that reach a maximum halfway through the
unroofing period (geotherm "b", A=0
mW/m3). Depending upon the assumptions
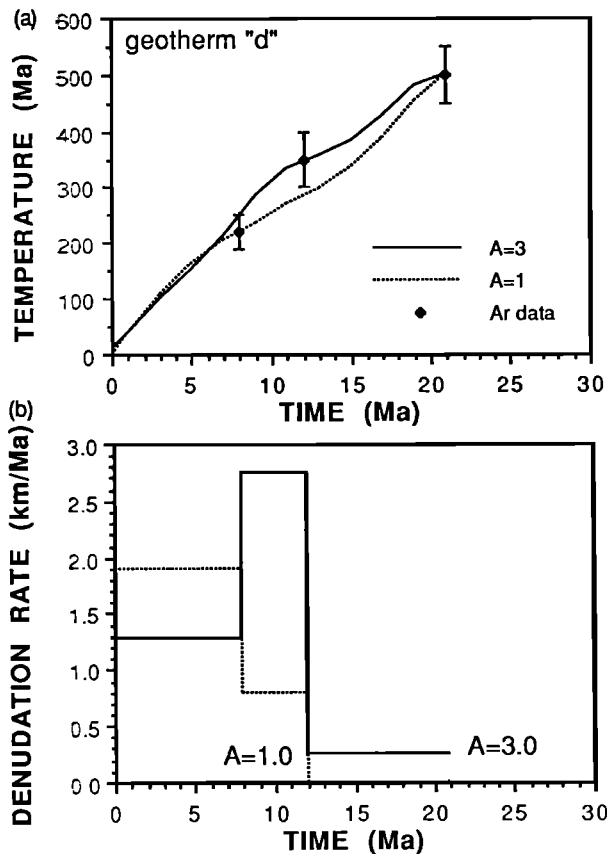made, the average unroofing rate between

Fig. 9. (a) T-t paths derived from initial geotherm "d", which models a source of cool temperatures at depth, for radiogenic heat production values of 1.0 and 3.0 μW/m3; (b) unroofing rates used to calculate the T-t paths shown in Figure 9a.

21 and 12 Ma may be as high as 2 km/m.y., or as low as 0 km/m.y. For the cases we examined it is at least possible to establish a lower bound of about 0.5 km/m.y. on the average unroofing rate between 12 and 0 Ma, although this result might not hold up if a broader range of thermal models were tested or if uncertainties in the observed geochronometers and thermobarometers were included in the analysis. The upper bound on unroofing rate over this time interval is poorly constrained even without including these uncertainties and must be at least 3 km/m.y.

Comparison of Figures 5-9 shows that, for a fixed value of radiogenic heat production but different initial geotherms, there is little difference between the model unroofing histories of the lower MCT zone. (Compare unroofing

histories for geotherms "a", "b", and "c" for fixed values of radiogenic heat production.) Therefore only a small part of the uncertainty in calculated unroofing histories can be attributed to uncertainties in the initial geotherm at depths structurally below the MCT. A greater contribution to the uncertainty in unroofing histories comes from uncertainties in the radiogenic heat production (Figures 5 and 6). However, by far the most important factors contributing to the uncertainty in calculated unroofing histories are the thermal boundary conditions in the lower crust and upper mantle following the cessation of thrusting on the MCT. Unfortunately, the thermal boundary conditions within the lower crust are poorly defined by observation, and it is probably not yet worthwhile to model them in detail. For example, although it is clear that movement on the MBT is responsible for advection of cold upper crustal material to depth below the MCT, we do not know if the structural depth of the MBT (or equivalent fault) has remained fixed with respect to the MCT, what the rate of displacement has been on this fault over the past 21 Ma, or how the geometry of the hanging wall wedge above the active MBT has changed with time (because much of the hanging wall has been eroded over the last 21 Ma).

The results of this study show clearly that one cannot simply translate cooling rate to unroofing rate within deeply eroded portions of thrust belts because the cooling history of a sample depends not only on its unroofing history but also on the thermal structure of the orogenic belt through time. Even if the geotherm were to remain unchanged through time, the cooling rate would be proportional to the unroofing rate only if the geotherm were linear with depth. Neither of these assumptions are reasonable in recently deformed and rapidly eroding orogenic belts. What is perhaps more surprising is that even when the initial geotherm is assumed to be constrained well by observational data from midcrustal depth, as in eastern Nepal, the time-dependent unroofing history of samples from midcrustal depth can be only poorly constrained by the use of cooling data. This should sound a cautionary note for geochronologic studies where unroofing rates are commonly estimated from cooling rates alone or where unroofing rates are

qualitatively equated with cooling rates.

What types of data would be needed to constrain unroofing histories and the evolving thermal structure of orogenic belts during erosion? Unroofing rates as a function of time are best constrained by PT data that describe the temperature-depth path of a single structural horizon during unroofing [e.g., Hodges and Royden, 1984], coupled with temperature-time data that describe the cooling history of the same structural horizon through time. By combining these data one can obtain a reasonable depth-time history. The evolving thermal structure of the orogen is more difficult to determine because of the difficulty in assigning realistic thermal boundary conditions to the lower crust or mantle lithosphere. However, through the use of (1) thermobarometric data for different structural horizons to establish an initial geotherm at mid to upper crustal depths, (2) petrologic data from different structural horizons to establish the temperature-depth path of the individual horizons through time, and (3) temperature-time data for the same structural horizon to chart their cooling histories one may obtain the best possible constraints on the thermal structure and the thermal boundary conditions within the lower crust and mantle lithosphere. It is probably only through the careful integration of such comprehensive quantitative data sets with theory and modeling of temperature structures that fundamental questions about thermal processes during orogenesis can ultimately be addressed.

REFERENCES

Bohlen, S. R., V. J. Wall, , and A. L. Boettcher, Experimental investigations and geological applications of equilibria in the FeO-TiO2-Al2O3-SiO2-H2O, Am. Mineral., 68, 1049-1058, 1983.

Bradbury, H. J., and R. C. Nolen-Hoeksema, The Lepontine Alps as an evolving metamorphic core complex during A-type subduction: Evidence from heat flow, mineral cooling ages, and tectonic modeling, Tectonics 4, 187-211, 1985.

Carnahan, B., H. A. Luther, and J. D. Wilkes, , Applied Numerical Methods, John Wiley, 604 pp., New York, 1969.

Carslaw, H. S., and J. C. Jaeger, Conduction of Heat in Solids, 2nd ed., 510 pp.,Oxford University Press, New York, 1959.

Copeland, P., T. M. Harrison, W. S. F. Kidd, R. Xu, and Y. Zhang, Rapid Early Miocene acceleration of uplift in the Gangdese belt, Xizang - southern Tibet, and its bearing on accomodation mechanisms in the India-Asia collision, Earth Planet. Sci. Lett., 86, 240-252, 1987.

England, P. C., and S. W.Richardson, The influence of erosion upon the mineral facies of rocks from different metamorphic environments, J. Geol. Soc. London, 134, 201-213, 1977.

England, P., and A. B. Thompson, Pressure-temprature-time paths of regional metamorphism, I. Heat transfer during the evolution of regions of thickened continental crust, J. Petrol., 25, 894-928, 1984.

Ferry, J. and F. S. Spear, Experimental calibration of the partitioning of Fe and Mg between garnet and biotite, Contrib. Mineral. Petrol., 66, 113-117, 1978.

Gansser, A., Geology of the Himalayas, 289 pp., Wiley Interscience, New York, 1964.

Gansser, A., The geodynamic history of the Himalaya, in Zagros, Hindu Kush, Himalaya Geodynamic Evolution, Geodyn. Ser., vol. 3,edited by H. K. Gupta and F. M. Delany pp. 111-121, AGU, Washington, D.C., 1981.

Harrison, T. M., Diffusion of 40Ar in hornblende, Contrib. Mineral. Petrol., 78, 324-331, 1981.

Harrison, T.M., and I. McDougall, Investigations of an intrusive contact, northwest Nelson, New Zealand I, Thermal, chronological and isotopic constraints, Geochim. Cosmochim. Acta, 44, 1985-2003, 1980.

Hodges, K. V., Pressure-temperature-time paths, Annu. Rev. Earth Planet. Sci., in press, 1991.

Hodges, K. V., and P. D. Crowley, Error estimation and empirical geothermobarometry for pelitic systems, Am. Mineral., 70, 702–709, 1985.

Hodges, K. V., and L. W. McKenna, Realistic propagation of uncertainties in geologic thermobarometry, Am. Mineral., 72, 673–682, 1987.

Hodges, K. V., and L. Royden, Geologic thermobarometry of retrograded metamorphic rocks: An indication of the uplift trajectory of a portion of the northern Scandinavian Caledonides, J. Geophys. Res., 89, 7077–7090, 1984.

Hodges, K. V., P. LeFort, and A. Pêcher, Possible thermal buffering by crustal anatexis in collisional orogens: Thermobarometric evidence from the Nepalese Himalaya, Geology, 16, 707–710, 1988.

Hubbard, M., Thermobarometry, $^{40}Ar/^{39}Ar$ geochronology, and structure of the Main Central Thrust zone and Tibetan Slab, eastern Nepal Himalaya, Ph.D. Thesis, 169 pp., Mass. Inst. of Technol., Cambridge, 1988.

Hubbard, M. S., Thermobarometric constraints on the thermal history of the Main Central Thrust zone and Tibetan Slab, eastern Nepal Himalaya, J. of Metamorph. Geol., 7, 127–134, 1989.

Hubbard, M. S., and T. M. Harrison, $^{40}Ar/^{39}Ar$ age constraints on deformation and metamorphism in the MCT zone and Tibetan Slab, eastern Nepal Himalaya, Tectonics, 8, 865–880, 1989.

Lyon-Caen, H. and P. Molnar, Gravity anomalies, flexure of the Indian plate, and the structure, support, and evolution of the Himalaya and Ganges Basin, Tectonics, 4, 513–538, 1985.

Molnar, P., Structure and tectonics of the Himalaya: Constraints and implications of geophysical data, Annu. Rev. Earth Planet. Sci., 12, 489–518, 1984.

Molnar, P., and P. England, Temperatures, heat flux, and frictional stress near major thrust faults, J. Geophys. Res., 95, 4833–4856, 1990.

Newton, R. C. and H. T. Haselton, Thermodynamics of the garnet-plagioclase-Al2SiO5-quartz geobarometer, in: Thermodynamics of Minerals and Melts, edited by R. C. Newton, A Navrotsky, and B. J. Wood, pp. 131–147, Springer-Verlag, New York, 1981.

Oxburgh, E. R., and D. L. Turcotte, Thermal gradients and regional metamorphism in overthrust terrains with special reference to the Eastern Alps, Schweiz. Mineral. Petrogr. Mitt., 54, 641–662, 1974.

Pinet, C., and C. Jaupart, A thermal model for the distribution in space and time of the Himalayan granites, Earth Planet. Sci. Lett., 84, 87–99, 1987.

Royden, L., and K. V. Hodges, A technique for analyzing the thermal and uplift histories of eroding orogenic belts: A Scandinavian example, J. Geophys. Res., 89, 7091–7106, 1984.

Zeitler, P. K., Cooling history of the NW Himalaya, Pakistan, Tectonics, 4, 127–151, 1985.

M. Hubbard, Department of Geological Sciences, University of Maine, Orono, ME 04469.

K. Hodges and L. Royden, Department of Earth, Atmospheric, and Planetary Sciences, Massachusetts Institute of Technology, Cambridge, MA 02139.